

High-pressure study of the Raman modes in $\text{YBa}_2(\text{Cu}_{0.96}\text{Ni}_{0.04})_4\text{O}_8$

D. J. Payne,* S. Guha,[†] Q. Cai, M. Chandrasekhar, and H. R. Chandrasekhar
Department of Physics, University of Missouri, Columbia, Missouri 65211

U. D. Venkateswaran
Department of Physics, Oakland University, Rochester, Michigan 48309

B. Jayaram and J. Ulanday
Materials Science Program, Department of Physics, University of Nebraska—Omaha, Omaha, Nebraska 68182
 (Received 5 March 1999)

We present a study of the Raman phonons in $\text{YBa}_2(\text{Cu}_{0.96}\text{Ni}_{0.04})_4\text{O}_8$ under hydrostatic pressure in the superconducting phase. A comparison with our earlier work on the undoped $\text{YBa}_2\text{Cu}_4\text{O}_8$ shows that the pressure coefficients of two vibrational modes involving oxygen atoms differ significantly from those of the corresponding modes in the undoped material. These are the O(1) chain mode which shifts 33% faster and the O(2)-O(3) in-phase mode which shifts 23% slower than the undoped counterparts. The other Raman modes in the Ni-doped sample shift in a manner similar to the undoped material. The observed behavior of the O(1) chain and O(2)-O(3) in-phase modes in $\text{YBa}_2(\text{Cu}_{0.96}\text{Ni}_{0.04})_4\text{O}_8$ under pressure and the softening of the Cu(1) A_g mode frequency with increasing Ni doping suggest that the Ni atoms substitute for the Cu atoms in the chain, which in turn decreases the compressibility in the vicinity of the Cu(Ni) chain atom. [S0163-1829(99)14429-1]

I. INTRODUCTION

The double Cu-O chain compounds $\text{YBa}_2\text{Cu}_4\text{O}_8$ (Y-124), where the chains are stacked along the c axis, have attracted a great deal of attention in recent years due to their excellent thermal stability¹ up to about 850 °C, in contrast to $\text{YBa}_2\text{Cu}_3\text{O}_7$ (Y-123), which becomes oxygen deficient between 350 and 400 °C. Since the chain atoms in Y-124 are not located at the center of inversion as in Y-123, phonons involving vibrations of chain atoms become Raman active. This is particularly advantageous in obtaining structural and dopant related information for Y-124 from the Raman spectrum. The interest in Y-124 is further enhanced by the large increase of T_c under hydrostatic pressure,^{2,3} $dT_c/dP = 0.55$ K/kbar, which is 10 times that of Y-123.

The substitution of Ni and Zn for Cu in Y-123 and Y-124 has been of special interest due to the fact that although Ni and Zn have similar chemical characteristics, nonmagnetic Zn suppresses T_c at a lower doping concentration than magnetic Ni. Information regarding the site occupancy of the dopant atom is important for understanding the difference in the suppression of superconductivity by Ni and Zn doping. Controversial data have been reported for the crystallographic site occupancy of Zn and Ni substituting for Cu. A direct determination of sites and bond lengths is rendered difficult due to the low contrast between neutron- or x-ray-scattering factors of Zn and Ni as compared with Cu. Much of the literature appears to favor the view that both Zn and Ni preferentially occupy the Cu(2) sites in the CuO_2 layers⁴⁻⁶ in the Y-123 materials, although the possibility of Zn at Cu(1) chain sites has also been discussed.⁷ With Ni doping, since the structure remains orthorhombic up to a solubility limit of 10 at. %, as is the case with Zn doping, it is believed that the Cu-O chains remain intact and that a substantial fraction of Ni goes into the CuO_2 planes, as it

does with Zn doping. Recently, we reported a Raman-scattering study⁸ of Ni- and Zn-doped Y-124, in which we found that Ni mainly substitutes for Cu in chain sites, unlike Zn which mainly substitutes for Cu in the plane sites. The different site occupancy may be the reason why superconductivity on doped Y-124 is destroyed more effectively by Zn than by Ni.

Raman scattering has been used effectively in high- T_c materials to probe the local environment of Cu and other dopant atoms substituting for Cu, as evidenced from the mode frequencies and their temperature and pressure dependence. There have been a few reports on the Raman spectra under pressure for Y-123 (Refs. 9–11) and Y-124 (Refs. 12–14). Boley *et al.*¹² have measured the mode Grüneisen parameters of the five chain and plane Raman modes in Y-124. Watanabe *et al.*¹³ have discussed the effect of pressure on the bonding sites in Y-124, focusing on the differences from the Y-123 system. Kakihana *et al.*¹⁴ measured the pressure dependence of seven Raman modes and found an anomalous behavior for the low-frequency Cu(2) mode. They suggested that this behavior indicates a change in the electronic state of the CuO_2 plane. So far, there has been no reported study of the high-pressure behavior of the Raman modes in doped Y-124. Since our recent Raman-scattering studies⁸ on Ni-doped Y-124 gave valuable insight into the site substitution of the dopants, we undertook a study of the Raman scattering in Ni-doped Y-124 under high pressure. The main motivation in this work is to observe how the local compressibility changes the environment near the substitutional sites and its effect on the vibrational modes.

II. EXPERIMENTAL DETAILS

Raman spectra are measured using triplemate spectrometer equipped with a liquid-nitrogen-cooled charge-coupled

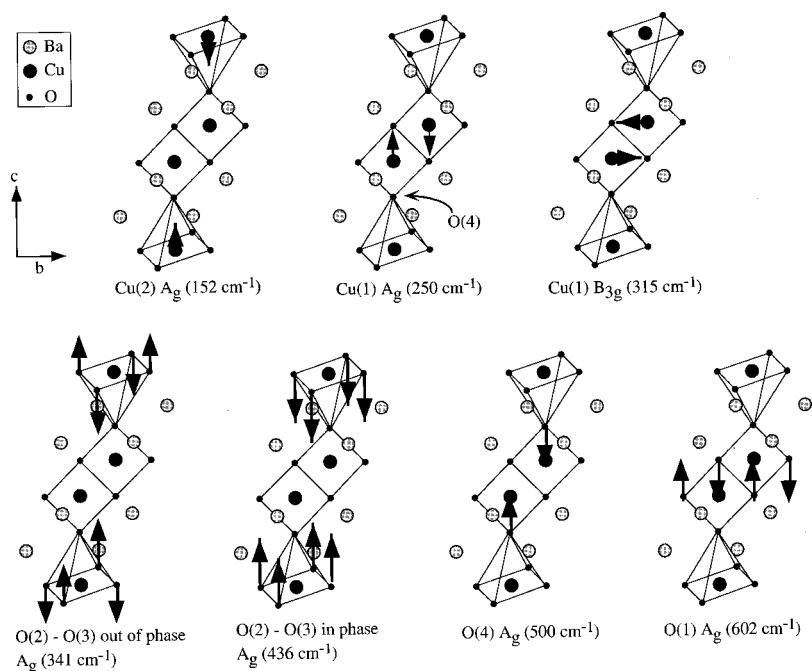


FIG. 1. Schematic representation of Raman-active lattice vibrations in Y-124.

device (CCD) detector and a holographic supernotch filter. Data were taken in the superconducting phase at 10 K with an instrumental resolution of about 3 cm^{-1} . Pressure studies are conducted in a Merrill-Bassett-type diamond anvil cell with cryogenically loaded argon as the pressure medium and ruby fluorescence as the manometer. About 10–15 mW of either the 488 or 514.5 nm line of an Ar^+ laser, focused to a spot size between 30 and $80 \mu\text{m}$, is used to excite the Raman spectra. Owing to the low scattering efficiency of the samples, it is necessary to use low-fluorescence diamonds and to divide out the diamond spectra in the pressure data. The resulting spectra are then fit to Lorentzian line shapes in order to obtain the peak frequency positions.

Samples of $\text{YBa}_2(\text{Cu}_{1-x}\text{Ni}_x)_4\text{O}_8$ are prepared by conventional solid-state reaction followed by high-pressure oxygen annealing. Appropriate quantities of Y_2O_3 , BaO, CuO, and NiO are thoroughly mixed and reacted in air for 24 h at 650, 750, and 880°C , respectively. The reacted powders are well mixed and cold pressed into pellets. These pellets are sintered at 950°C and annealed at 500°C in oxygen for 16 h. The sintered ceramic samples are finally annealed at 990°C for 48 h (in a Morris Research model HPD-5010P furnace) under an oxygen pressure of 100 bars.

A Rigaku x-ray diffractometer with Cu $K\alpha$ radiation is used to record powder diffraction patterns at room temperature. Silicon is used as an internal standard to follow the shifts in peak positions due to substitution at the Cu site. Lattice parameters are determined from least-squares fits to the diffraction lines indexed with the space group $Ammm$. There is no change in the lattice parameters⁸ within a scatter of $\pm 0.1\%$. dc magnetic susceptibility measurements are made using Quantum Design superconducting quantum interference device (SQUID) magnetometer in the “field-cooled” mode in an external field of 10 G. The superconducting transition temperature (T_c) where the onset of diamagnetic signal is observed is found to be 34 K for the $\text{YBa}_2(\text{Cu}_{0.96}\text{Ni}_{0.04})_4\text{O}_8$ sample used in this study.

III. RESULTS AND DISCUSSION

Figure 1 shows schematically the motion of atoms for the observed Raman-active vibrational modes. We note that there are three Cu and four O modes associated with the various copper and oxygen atoms in the unit cell. The frequencies of the Raman modes in Ni-doped Y-124, obtained after Lorentzian fits to the Raman line shapes, are plotted as a function of Ni concentration in Fig. 2, where the left and right panels are for the Cu and O modes, respectively. Similar plots of our preliminary data have been published earlier.⁸ The mode frequencies reported in Ref. 8 were read off the spectra in contrast to the Lorentzian line shape fits used for the data in Figs. 2(a) and 2(b). Thus the results presented here are more accurate. We note that the change in the O mode frequencies over the 5% Ni doping range is rather small, $0.5\text{--}2.5 \text{ cm}^{-1}$ (right panel in Fig. 2). On the other hand, the frequency of the A_g Cu(1) chain mode at 260 cm^{-1} in the undoped Y-124 softens by about 13 cm^{-1} in the range 0–5% of Ni substitution. This softening is seen both in the normal and superconducting phases.⁸ In contrast, the B_{3g} mode of the same Cu(1) atom (315 cm^{-1}) experiences virtually no shift in frequency, indicating little change in the force constants along the b direction upon doping. The in-plane Cu(2) mode (152 cm^{-1}) exhibits a small softening of about 3 cm^{-1} between 0% and 2% Ni doping, beyond which it recovers to the original 0% value. The large shift in the Cu(1) A_g mode frequency over a small range of Ni concentrations clearly indicates that a substantial fraction of Ni atoms occupy the chain Cu(1) site. The frequency softening is found to saturate around 4–5% Ni doping, indicating that for higher values of Ni doping, a large fraction of the Ni does not go into the substitutional sites, but accumulates at the grain boundaries. The 5% decrease in the frequency of the Cu(1) mode cannot be accounted for in any simplistic harmonic oscillator model involving changes of masses alone. Hence we conclude that the force constants and the local

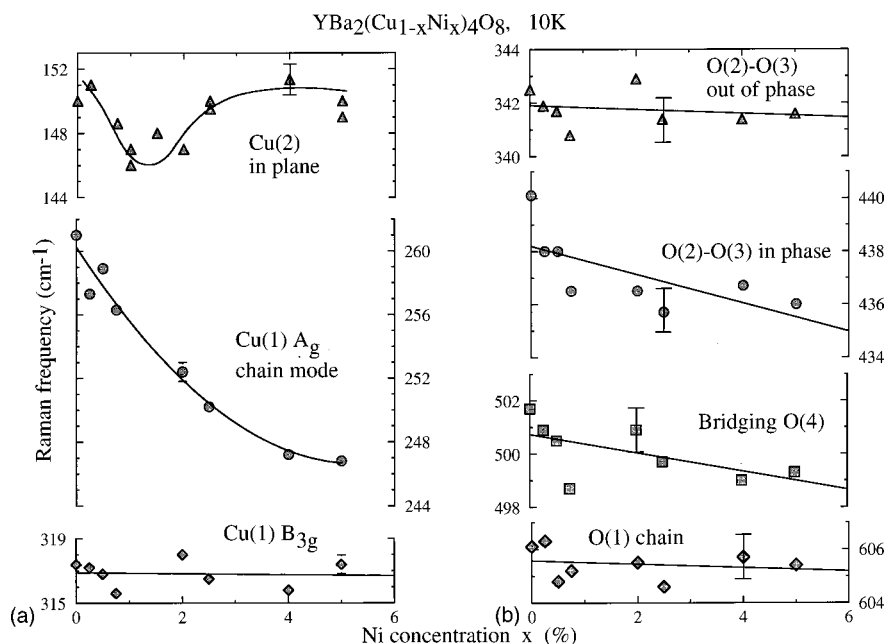


FIG. 2. Frequencies of the Raman modes associated with Cu atoms (a) and O atoms (b) as a function of Ni concentration x . The Cu(1) A_g chain mode softens considerably with increasing Ni doping, whereas all other modes exhibit small or no shifts in their frequency. The line through the B_{3g} mode frequencies is a guide to the eye. Lines through the Cu(1) A_g and Cu(2) mode frequencies are fits to a second-order polynomial and a linear function, respectively.

compressibility around the Ni atom in the chain site have been reduced.

The small change in the Cu(2) in-plane mode frequency as compared to the large change in the Cu(1) chain mode does not completely rule out the possibility of Ni substitution in the planes. It is likely that Ni substitutes for Cu in both the chain and planes. The chain and plane Cu atoms are in different crystalline environments, which results in different hybridization of their electronic states. The asymmetric bonds in the Cu(1) A_g vibration as compared with the symmetric bonds in the CuO_2 planes could preferentially change force constants and frequencies of the chain mode.

Studies of the bond lengths and possible distortions in Ni-doped Y-123 have been investigated using extended x-ray-absorption fine structure (EXAFS).¹⁵ These studies indicate that in a sample with $x = 0.033$, both Cu(1) and Cu(2) sites are occupied by Ni and that, to within 15%, the occupancy is uniform. These measurements show that the Ni(1) sites appear undistorted, while there is some distortion around the Ni(2) sites. The Ni(2)-O(4) and Ni(2)-Y bond lengths are slightly longer (5.2% and 2%, respectively), while the Ni(2)-Ba bond is 1.5% shorter. The Ni(1)-O(4) bond distance remains the same, as do the Ni(1)-Ba and Ni(2)-O(2) bonds. While EXAFS gives the bond lengths, it does not provide an indication of the bond's compressibility, which reflects the local environment via the Coulombic force constants.

As the results presented in Fig. 2 show a clear indication of changes in the local compressibility around the chain sites, it is interesting to study the pressure dependence of the vibrational modes in Ni-doped Y-124. We chose a sample with $x = 0.04$, for which the doping-induced frequency shift and also the Raman signal are high. This sample also represents a concentration at which the frequency shift is close to the saturation value. Raman modes in this sample are studied

in the superconducting phase (at 10 K) under hydrostatic pressure conditions over a range of 0–80 kbar. Vibrations corresponding to the Cu(1) A_g mode at 248 cm^{-1} , Cu(1) B_{3g} mode at 315 cm^{-1} , O(2)-O(3) out-of-phase A_g mode at 342 cm^{-1} , O(2)-O(3) in-phase A_g mode at 438 cm^{-1} , O(4) apical oxygen A_g mode at 500 cm^{-1} , and O(1) chain A_g mode at 605 cm^{-1} are followed under pressure at 10 K. The Cu(1) mode at 146 cm^{-1} could not be observed due to the large Rayleigh scattering of the ceramic samples within the diamond anvil cell.

Since our studies are conducted in the superconducting phase, it is important to know the temperature-induced frequency shifts of the Raman mode, in particular to ensure that pressure data are being acquired in a temperature range where there is no steep change in the frequency for any of the modes. The temperature dependence of the mode frequencies at 1 bar is shown in Fig. 3. All modes show a hardening that commences at 60 K and flattens at $T_c = 34 \text{ K}$. We have found this hardening to be typical of many of the Ni-doped samples, with the exception for some of the modes that will be discussed in a different publication. We notice that the frequency remains flat in the region between 10 K and T_c for all modes. With the application of pressure, if the T_c of this sample increases, as is typical of pure Y-124, the temperature-dependent frequency changes which occur above T_c (see Fig. 3) would only be shifted to higher temperature and therefore should not affect our measurements, all of which are carried out at 10 K.

The Raman spectra under pressure are shown in Fig. 4. We find that, despite weak signals, all peaks except the 146 cm^{-1} mode are observed up to 80 kbar. The linewidths of the peaks are seen to increase slightly with pressure, indicating an inhomogeneity of about 2 kbar at the highest pressures. The 1 bar spectrum shows a broad background that extends

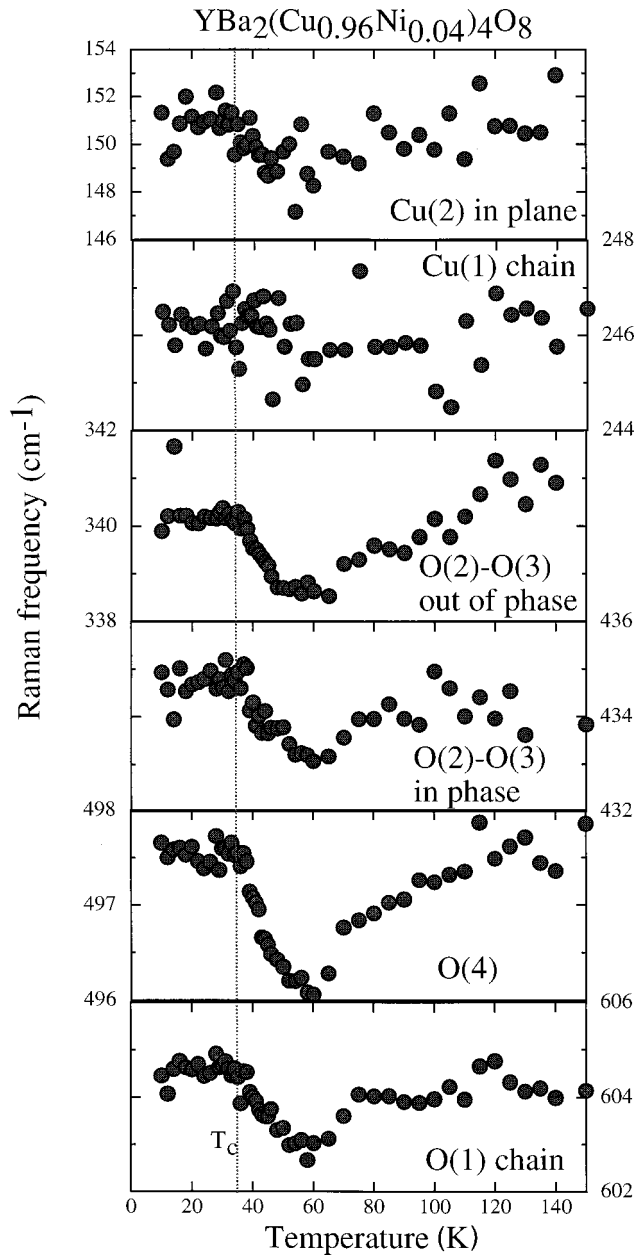


FIG. 3. Temperature dependence of the frequencies of Raman modes in $\text{YBa}_2(\text{Cu}_{0.96}\text{Ni}_{0.04})_4\text{O}_8$ at 1 bar. The dotted line at 36 K represents T_c for this sample.

from 200 to 700 cm^{-1} . This background does not change substantially in either shape or intensity with temperature over the 10–150 K range. Since our samples are ceramics, we conclude that the background arises due to the luminescence from impurities and inclusions. The relative magnitude of this background does not change much with pressure either, although it appears to be more pronounced in the 200–400 cm^{-1} range at higher pressure, making the Cu(1) and O(2)-O(3) modes appear superimposed on a broad peak. Furthermore, peaks in the 500–700 cm^{-1} range are seen to ride on a sloping background at high pressures.

The frequencies of all modes increase linearly with pressure and can be fit to $\omega(P) = \omega(0) + (d\omega/dP)P$, where P is in kbar and ω is in cm^{-1} . The pressure shifts of the Raman modes in the superconducting state of the Ni-doped sample studied here and those of the undoped Y-124 studied

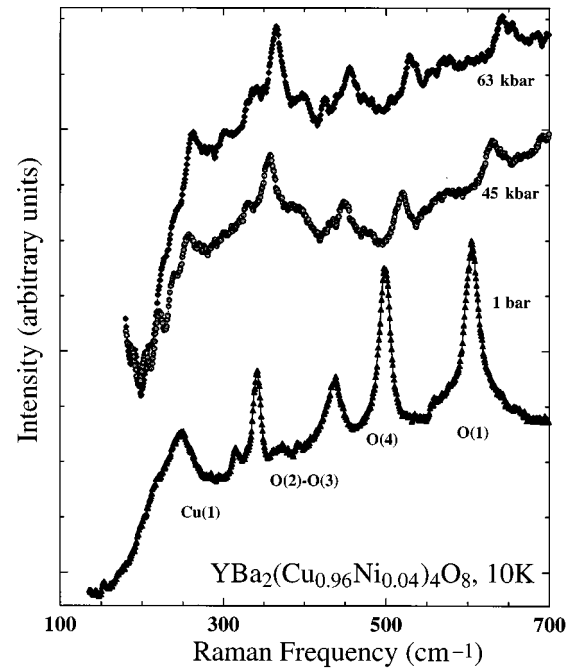


FIG. 4. Raman spectra of $\text{YBa}_2(\text{Cu}_{0.96}\text{Ni}_{0.04})_4\text{O}_8$ under pressure.

earlier¹² are summarized in Table I. Also included in this table are the pressure coefficients obtained in other works^{13,14} at room temperature (normal state) for undoped Y-124. We first compare the frequency shifts obtained in our works in the superconducting state of Ni-doped and undoped Y-124 (columns 4 and 5 in Table I). We find that for several of the modes such as the Cu(1) mode, the B_{3g} mode, the O(2)-O(3) out-of-phase mode, and the O(4) apical mode, the pressure-induced frequency shifts are very similar whereas two other modes, viz., the O(2)-O(3) in-phase mode and the O(1) chain mode, stand out in their dissimilarity.

The O(1) chain mode in doped Y-124 shows a 33% increase in its pressure coefficient when compared to undoped Y-124, namely, $0.56 \text{ cm}^{-1}/\text{kbar}$ in Ni-doped Y-124 at 10 K as compared to $0.42 \text{ cm}^{-1}/\text{kbar}$ previously reported¹² for undoped Y-124 in the superconducting state. In contrast, the pressure coefficient for the O(2)-O(3) in-phase mode is 23% lower in the doped material than that for undoped Y-124, namely, $0.33 \text{ cm}^{-1}/\text{kbar}$ in the 4% Ni-doped Y-124 as compared to a value of $0.43 \text{ cm}^{-1}/\text{kbar}$ in the undoped sample. In comparison the pressure coefficients of all other modes in the undoped and 4% Ni-doped Y-124 agree within their uncertainties. Clearly, the observed changes in the pressure coefficients of the O(2)-O(3) in-phase mode and the O(1) chain mode in the Ni-doped Y-124 are not coincidental.

These differences in pressure coefficients are seen in more detail in Fig. 5, where we plot the frequency of the O(1) chain and O(2)-O(3) in-phase modes as a function of pressure. Solid circles represent current data for 4% Ni-doped Y-124 at 10 K and open squares denote data for undoped Y-124 and 14 K taken from Ref. 12. Solid lines through the data are linear least-squares fits. It can be seen from these plots that there is a clear difference in the pressure coefficient of these two modes in the 4% Ni-doped sample compared to the undoped sample. In this context it might be interesting to investigate a series of samples with different Ni concentra-

TABLE I. Pressure shift of Raman modes in Ni-doped and undoped Y-124.

Mode	Assignment	ω_0 (cm^{-1}) [10 K]	Ni-doped	Undoped	Undoped	Undoped
			Y-124 [10 K] (current work)	Y-124 [14 K] (Boley <i>et al.</i>) ^a	Y-124 [300 K] (Watanabe <i>et al.</i>) ^b	Y-124 [300 K] (Kakihana <i>et al.</i>) ^c
A_g	Cu(2)	146			0.22 ± 0.02	0.31 ± 0.03^d
A_g	Cu(1)	248	0.23 ± 0.03	0.27 ± 0.03	0.25 ± 0.02	0.22 ± 0.02
B_{3g}	Cu(1)	315	0.34 ± 0.03		0.33 ± 0.02	0.30 ± 0.04
A_g	O(2)-O(3)	342	0.34 ± 0.03	0.34 ± 0.03	0.35 ± 0.03	0.32 ± 0.01
	out-of-phase					
A_g	O(2)-O(3)	438	0.33 ± 0.03	0.43 ± 0.03	nonlinear	
	in-phase					
A_g	O(4)	500	0.52 ± 0.03	0.54 ± 0.03	0.45 ± 0.02	0.38 ± 0.02
A_g	O(1)	605	0.56 ± 0.03	0.42 ± 0.03	0.50 ± 0.02	0.49 ± 0.04

^aReference 12.^bReference 13.^cReference 14.^dLinear fit up to 55 kbar; nonlinearity was seen above 60 kbar.

tions in a future study. A comparison of the frequency versus pressure graphs in Ni-doped and undoped Y-124 for the remaining four modes is shown in Fig. 6. It is evident that the pressure behavior of these modes is very similar in the doped and undoped samples.

An analysis of the $\text{YBa}_2\text{Cu}_4\text{O}_8$ unit cell reveals how the response of the lattice to pressure is governed by the local bonds around each atom. Atomic vibrations are sensitive to bond-bending and bond-stretching force constants. Coulomb force constants for bond bending are approximately one-half that of bond stretching. Thus one would expect c -axis bond stretching vibrations to be more strongly affected by pressure because the c -axis compressibility is the largest. In comparing the Ni-doped to undoped Y-124, vibrations that involve Ni-O bond stretching should be affected more than the modes involving bond bending. Thus, as shown in Fig. 1, the Cu(1) B_{3g} mode at 315 cm^{-1} with vibrations along the b axis and O(2)-O(3) out-of-phase mode at 342 cm^{-1} which primarily involves bond bending in the Cu-O plane should not be

affected by Ni chain substitution. We find this to be the case indeed with the O(2)-O(3) out-of-phase mode (Table I and Fig. 6), although the B_{3g} mode in the undoped sample was too weak to follow under pressure.

That leaves four c -axis modes, viz., the Cu(1) chain mode, O(2)-O(3) in-phase, O(4) apical mode, and O(1) A_g mode. We first discuss the 248 cm^{-1} Cu(1) chain mode which has an O(1) as its neighbor on one side with a bond length of 1.88 \AA and an O(4) on the other side with a bond length of 1.84 \AA along the c axis (see Fig. 1). We recall that this is the mode whose frequency (and consequently the local force constant and compressibility) is affected by a large amount by Ni doping (Fig. 2), indicating that Ni substitutes for Cu(1) in the chain position. Under pressure, however, its frequency shift is close to that of the undoped material. Apparently, the positioning of Cu(1) between four oxygen atoms O(4) and O(1), one on each side along the c axis, and two O(1)'s, one on each side along the b axis, holds the atom with sufficient rigidity that even higher compressibility along

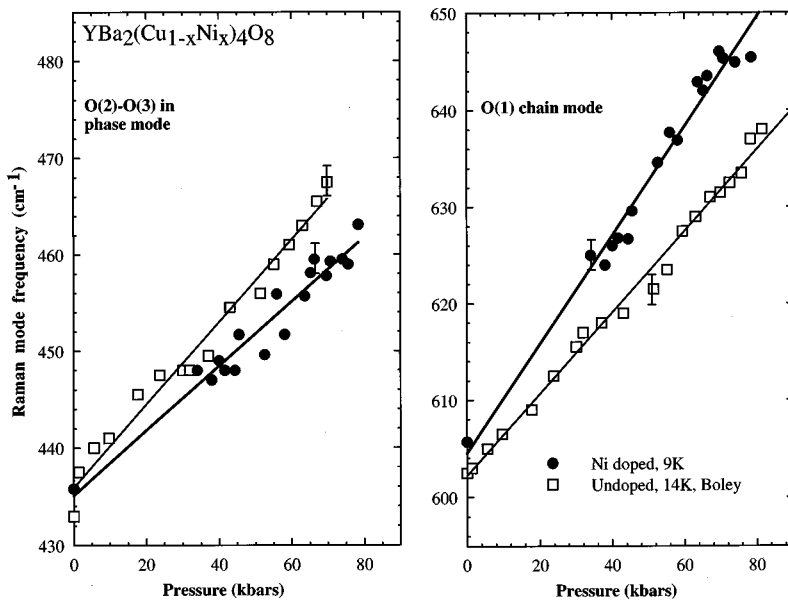


FIG. 5. Pressure-induced shifts in the frequency of the in-phase and chain modes of oxygen. Current work (solid line) is compared to previous work on undoped sample (Ref. 12) (open symbols).

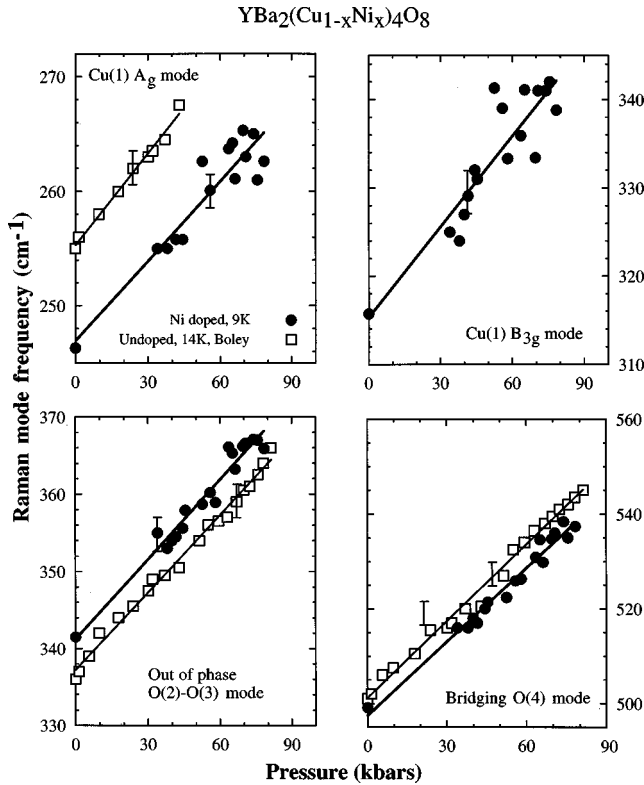


FIG. 6. Pressure-induced shifts in the frequencies of the Cu(1) A_g , Cu(1) B_{3g} , out-of-phase O(2)-O(3), and O(4) bridging modes. These modes show similar pressure shifts regardless of whether they are doped or undoped.

the Ni-O bond does not cause its pressure-induced frequency shift to vary greatly from that of undoped $\text{YBa}_2\text{Cu}_4\text{O}_8$. Furthermore, the Cu(1)-O(1) bonds along the b axis are more rigid and hence allow a minimal effect on those bonds by changes in the c axis. The small linear compressibility along the b axis ($1 \times 10^{-3}/\text{GPa}$) is the key quantity that holds the Ni/Cu(1) rigid and unaffected by an increased compressibility along the c axis. In comparison, the linear compressibility along the a and c axes is $2.8 \times 10^{-3}/\text{GPa}$ and $5.5 \times 10^{-3}/\text{GPa}$, respectively.¹⁶

The second mode we discuss is the one at 500 cm^{-1} which is assigned to the O(4) apical mode with an O(1) on one side and a Cu(2) on the other. This vibration involves stretching of the long and weak Cu(2)-O(4) bond (length = 2.29 \AA) and the bending of the O(4)-O(2) and O(4)-O(3) bonds in the CuO_2 plane. In addition, it involves the bending of the O(1)-O(4) bond (length = 2.78 \AA) between the chain and plane. Since the O(4) is bonded to several neighbors, most of which are oxygen atoms, one would not expect it to be affected appreciably by Ni substitution of the one Cu(1) atom, even though that bond is the shortest. Indeed, the pressure coefficients for this mode in the doped and undoped samples are the same at low temperature within the experimental error (Table I).

Of the remaining modes involving c -axis vibrations, the 605 cm^{-1} O(1) chain mode has a short bond to the Cu(1) on the one side and to the rather distant O(2) atom in the CuO_2 plane along the c direction. The 438 cm^{-1} O(2)-O(3) in-phase mode vibrates against the O(1) on the one side along c and another O(2)-O(3) plane on the other side, both of which

are rather large distances compared to, say, the Cu(1)-O(1) bonds. It is these two modes that show the largest deviation of pressure coefficients from the pristine sample. The in-phase mode has a smaller pressure coefficient, while the chain mode has a large pressure coefficient in the doped material as compared to the undoped sample.

If the Coulomb force constant between Ni-O becomes smaller than that between Cu-O, it would decrease the frequency of the Cu(Ni) mode, as has been observed, and also make the bond more compressible. This, in turn, should increase the frequency of the associated mode faster than that of a stiffer bond owing to the rapid decrease in the related bond length. Indeed, this is what we observe: the O(1) mode frequency increases faster with pressure in the Ni-doped material than it does in the pristine sample.

While the Cu(1)-O(1) bond compresses faster under pressure, it has the relative effect of stretching the O(2)-O(1) bond, which comes into picture for the O(2)-O(3) in-phase mode vibrations which are along the c axis. The net effect of the increase in the O(2)-O(3) bond length is to decrease the force constant and thus cause the frequency of the in-phase mode to change more slowly than in the undoped material.

The presence of Ni in the chain sites, which are considered the charge reservoirs, could affect the charge transfer mechanism differently from its presence in a plane site.¹⁷ The O-Cu-O network in the charge reservoir may not function as effectively with Ni in random positions. Indeed, the destruction of superconductivity may occur less effectively due to Ni in chain sites than in plane sites and thus provide an additional mechanism for the lack of suppression of T_c with Ni doping.

It is interesting to compare the pressure coefficients of the Raman modes measured in the superconducting state¹² of undoped Y-124 with those reported by two other groups^{13,14} in the normal state. We note that there is an overall agreement (within the experimental error bars) between the pressure-induced frequency shifts of the low-frequency ($<350 \text{ cm}^{-1}$) modes in the normal and superconducting sites (see Table I). The O(2)-O(3) in-phase mode (at $\sim 438 \text{ cm}^{-1}$) was not studied under pressure in Ref. 14 due to its weak intensity and in the work of Watanabe *et al.*¹³ the frequency shift of this mode saturates about 60 kbar and the peak splits into two peaks around 80 kbar. This nonlinear pressure behavior in the normal state is in sharp contrast to the linear pressure shift up to 70 kbar observed in our study of the superconducting state (see Table I and Fig. 5). In the case of the O(4) mode (at $\sim 500 \text{ cm}^{-1}$), the two values reported for the pressure shift in the normal state^{13,14} do not agree within their standard deviation and are both lower than the value determined in the superconducting state. The pressure shift of the O(1) mode frequency is lower in the superconducting state than that in the normal state. Although it is tempting to correlate the differences observed in the normal and superconducting states for the pressure derivatives of the bridging O(4) and chain O(1) mode frequencies to the origin of superconductivity in Y-124, definite conclusions can be made only when the same sample is studied in the normal and superconducting states. However, the main observation in this study, viz, in the 4% Ni-doped Y-124, the O(1) chain mode shifts faster, the O(2)-O(3) in-phase mode shifts

slower than their undoped counterparts, is valid since it is meaningful to compare the measurements made by the same group in the superconducting states of both these samples.

IV. CONCLUSIONS

Motivated by our earlier study⁸ that showed a substantial change in the Cu(1) mode frequency as a function of Ni doping in Y-124, a hydrostatic pressure study was conducted on a 4% Ni-doped sample in the superconducting state. We originally expected the Cu(1) mode to shift differently in the Ni-doped material with pressure, but found that the rigidity of the *b*-axis bonds overcomes the higher compressibility along the short *c*-axis bonds. However, two other modes, namely, the O(1) and O(2)-O(3) in-phase modes, that vibrate against the Ni/Cu(1) bond are affected by Ni doping in the chain sites. The higher Cu(1)-O(1) bond compressibility has the effect of increasing the rate at which the frequency of the O(1) chain mode hardens under pressure than is the case with the corresponding mode in pristine Y-124. This higher compressibility results in the relative stretching of the O(1)-O(2) bond, making the O(2)-O(3) in-phase mode frequency to increase slower under pressure in the Ni-doped Y-124 as compared to undoped Y-124. The remaining modes exhibit pressure dependences similar to those reported for undoped Y-124. The differences and similarities in the pressure shifts

of the Raman modes in the Ni-doped and undoped Y-124 are understood in terms of the local environment around each atom. The response of the O(2)-O(3) in-phase mode and the O(1) chain mode also support our earlier suggestion of the chain occupancy for Ni.

The question of how Ni affects the superconducting transition temperature is still an open one. Charge transfer from the charge reservoirs (the chains) to the CuO₂ planes is clearly affected by the substitution of Ni into the chains. Moreover, this charge transfer will be affected by hydrostatic pressure, and the pressure coefficient of T_c , dT_c/dP , will be affected by Ni doping. There should be two opposing mechanisms that will affect dT_c/dP : the decreased charge transfer due to Ni in the Cu(1) site and the increased efficiency of charge transfer under pressure due to the higher *c*-axis compressibility. At present, we are not aware of studies of dT_c/dP in Ni-doped Y-124 and are therefore unable to say which of the two mechanism wins out.

ACKNOWLEDGMENTS

This work was supported by U.S. Department of Energy Grant No. DE-FG02-90ER45427 through the Midwest Superconductivity Consortium. D.J.P. thanks the U.S. Department of Education for support through Grant No. P200A50259.

*Present address: Duke University, 131 Environmental Safety Building, Box 3914, Durham, NC 27710.

[†]Present address: Department of Physics, Marquette University, Milwaukee, WI 53201.

¹J. Karpinski, E. Kaldis, E. Jilek, S. Rusiecki, and B. Bucher, *Nature (London)* **336**, 660 (1988).

²B. Bucher, J. Karpinski, E. Kaldis, and P. Wachter, *Physica C* **157**, 478 (1989).

³J. J. Scholtz, E. N. van Eenige, R. J. Wijngaarden, and R. Griessen, *Phys. Rev. B* **45**, 3077 (1992).

⁴H. Yamagata, K. Inada, and M. Matsumura, *Physica C* **185–189**, 1101 (1991).

⁵H. Maeda, A. Kocuzumi, N. Bamba, E. Takayama-Muromachi, F. Izumi, H. Asano, K. Shimizu, H. Morimaki, H. Murayama, Y. Kuroda, and H. Yamazaki, *Physica C* **157**, 483 (1990).

⁶H. Shaked, J. Faber, B. W. Veal, R. L. Hitterman, and A. P. Paulikas, *Solid State Commun.* **75**, 445 (1990).

⁷P. Mendels, *Physica C* **171**, 429 (1990).

⁸D. J. Payne, M. Chandrasekhar, H. R. Chandrasekhar, B. Jayaram, and J. Ulanday, *Solid State Commun.* **98**, 971 (1996).

⁹K. Syassen, M. Hanfland, K. Strossner, M. Holtz, W. Kress, M.

Cardona, U. Schroder, J. Prade, A. D. Kulkarni, and F. W. de Wette, *Physica C* **153–155**, 264 (1988).

¹⁰D. Kulakovskiy, O. V. Misochko, V. B. Timofeev, M. I. Erements, E. S. Itskevich, and V. V. Struzhkin, *Pis'ma Zh. Eksp. Teor. Fiz.* **47**, 536 (1988) [*JETP Lett.* **47**, 626 (1988)].

¹¹A. F. Goncharov, M. R. Muinov, T. G. Uvarova, and S. M. Stishov, *Pis'ma Zh. Eksp. Teor. Fiz.* **54**, 113 (1991) [*JETP Lett.* **54**, 111 (1991)].

¹²M. S. Boley, M. Chandrasekhar, H. R. Chandrasekhar, Y. Wu, and P. Boolchand, *High Pressure Science and Technology—1993*, edited by S. C. Schmidt *et al.*, AIP Conf. Proc. No. 309 (AIP, New York, 1994), p. 681.

¹³N. Watanabe, M. Kosuge, N. Koskizuka, S. Adachi, and H. Yamauchi, *Phys. Rev. B* **49**, 9226 (1994).

¹⁴M. Kakihana, H. Arashi, M. Yashima, M. Yoshimura, L. Börjesson, and M. Käll, *Physica C* **230**, 199 (1994).

¹⁵F. Bridges, J. B. Boyce, T. Claeson, T. H. Geballe, and J. M. Tarascon, *Phys. Rev. B* **42**, 2137 (1990).

¹⁶H. A. Ludwig, W. H. Fietz, M. R. Dietrich, H. Wühl, J. Karpinski, E. Kaldis, and S. Rusiecki, *Physica C* **167**, 335 (1990).

¹⁷S. L. Cooper, F. Slakey, M. V. Klein, J. P. Rice, E. D. Bukowski, and D. M. Ginsberg, *Phys. Rev. B* **38**, 11934 (1988).